**ISSN 1840-4855**
**e-ISSN 2233-0046**

**Original scientific article**
**http://dx.doi.org/10.70102/afts.2025.1834.431**

# HYBRID SOLAR-WIND INTEGRATION USING AN ADAPTIVE NETWORK RECONFIGURATION METHOD AND CONTROLLING FOR UNCERTAINTY-AWARE SMART GRID BY OPTIMIZATION ALGORITHM

Ghaith M. Fadhil[1*], Saeid Ghassem Zadeh[2]

*[1*]Faculty of Electrical and Computer Engineering, University of Tabriz, 29 Bahman boulevard, Tabriz, Iran; Civil Engineering Department, College of Engineering, Al-Qasim Green University, Babylon, Iraq. e-mail: ghaith.maged@tabrizu.ac.ir, orcid: https://orcid.org/0009-0006-0675-1456*
*[2]Faculty of Electrical and Computer Engineering, University of Tabriz, 29 Bahman boulevard, Tabriz, Iran. e-mail: g_zadeh@tabrizu.ac.ir, orcid: https://orcid.org/0000-0002-2389-3521*

***Received: September 04, 2025; Revised: October 18, 2025; Accepted: November 25, 2025; Published: December 30, 2025***

SUMMARY

In this work, a new optimization approach for the exploitation and smooth integration of hybrid renewable sources (HRs), including PV solar/wind turbines in addition to a dynamic reconfiguration process of electricity distribution microgrids, is proposed. A crucial novelty of this work is the definition of a multi-scenario optimization framework that allows to compare devices at various levels (of complexity) across different system conditions, and which has not been thoroughly investigated yet in the literature. Further, the study presents one of the most detailed and operational-realistic representations of an IEEE 84-bus Taiwan Power Company (TPC) distribution system model (in a unique dataset containing exact switch status, impedance properties, and power injection location). This network model serves as a scalable benchmark for grid optimization studies and utility-scale PV deployment. Moreover, the proposed method adopts a variant of particle swarm optimization algorithm to minimize the operational cost along with the variance-based penalty function in consideration of uncertainty associated with renewable power generation. This combination of cost effectiveness and uncertainty management in the context of a single objective function increases the stability and flexibility in grid functions. Then, the approach is verified for three operational modes: a base scenario without any renewable integration, a PSO-tuned scenario with PV and WT but ignoring network reconfiguration, and an integrated (renewables together with reconfiguration). The final formation achieved after optimization can minimize the power losses from 4.924 MW to around 0.002 MW and reduce the operational cost to $1.954/MWh, as reported in results. Such results validate the effectiveness of our proposed strategy for facilitating cost-efficient and robust operation of smart grid.

Key words*: renewable energy integration, IEEE 84-bus system, multi-scenario simulation, network reconfiguration, optimization algorithm, uncertainty modeling.*

Table 1: List of signs and symbols

| List of signs and symbols | | | |
|---|---|---|---|
| $C_i(x_i)$ | *Cost function for each microgrid or participant* | $p$ | *Air density* |
| $\lambda$ | *Weight factor for uncertainty variance penalty* | $v$ | *Wind speed* |
| $Var(\Delta P_{RE})$ | *Variance of the uncertainty in renewable energy* | $C_p$ | *Turbine power factor* |
| $\eta_{PV}$ | *Efficiency of the PV module* | $P_{k,t}^{net}$ | *Represent the power flow in the reconfigurable network.* |
| $A$ | *Area of the PV module* | $P_{ik,t}$ | *Active power flow from node i to node k at time t.* |
| $G$ | *Solar irradiance (W/m²)* | $\gamma_{ik,t}$ | *A binary variable (0 or 1) related to the status of the connection or line between node i and node k at time t* |
| $\theta$ | *Angle of incidence of sunlight on the panel* | $Q_{k,t}^{net}$ | *Net reactive power at node k at time t.* |
| $U_{k,t}$ | *Voltage magnitude at bus k at time t.* | $Q_{ik,t}$ | *Reactive power flow from node i to node k at time t.* |
| $U_{i,t}$ | *Voltage magnitude at bus i at time t.* | $x_{ik}$ | *Reactance of the line/branch connecting bus i to bus k. This is also typically a fixed parameter of the line.* |
| $r_{ik}$ | *Resistance of the line/branch connecting bus i to bus k. This is typically a fixed parameter of the line.* | $U_i^{min}$ | *Minimum permissible voltage magnitude at bus i.* |
| $C_{i,t}^{Gen}$ | *Total generation cost for component i at time t.* | $U_i^{max}$ | *Maximum permissible voltage magnitude at bus i.* |
| $\lambda_i^{MT}$ | *Cost coefficient (or price) for electricity generated by a specific type of generator MT* | $H_{i,t}^{TSC}$ | *Capacity or amount related to "TS"* |
| $\lambda_i^{BS}$ | *Cost coefficient (or price) for buying/selling electricity from a specific "BS" source* | $k_i^{TS}$ | *Cost coefficient (or penalty) related to "TS"* |
| $H_{i,t}^{TSD}$ | *Demand or discharge related to "TS"* | $r_1$ *and* $r_2$ | *takes values randomly between 0 and 1.* |
| $v_i^{(t+1)}$ | *the particle's velocity* | $p_i^{best}$ | *best particle found position* |
| $w$ | *factor that determines how long the current motion will continue based on the previous velocity.*$c_1$ *and* $c_2$ *are acceleration coefficients* | $g^{best}$ | *position of the swarm* |
| $x_i^{(t)}$ | *the position of particle number "i" at time instant (t).* | $v_i^{(t+1)}$ | *velocity of particle"i" at the next time instant* $(t+1)$ |

Table 1 provides the different signs, symbols, and their respective definitions that are applied throughout the paper in the description of important parameters of optimizing the hybrid solar-wind integration in smart grids. These are symbols that form part of the mathematical and operation structure such as variables of power flow, energy generation and optimization methods used in the system.

## INTRODUCTION

### Motivation

With the increase of distributed generators in power grid, e.g., photovoltaic (PV) and wind turbines (WT) [1], [2], the modern electrical systems need DERs as the cornerstones. Rationalizing trading and transactions in modern, decentralized smart microgrids using advanced energy trading algorithms. For stability, sustainability, energy independence and perfectly efficient energy trading with the grid, the optimal distribution is necessary at all times which is referred to as Network Reconfiguration (NR) [3], [4]. NR is a pivotal process, which transmits and exchanges or redistributes the power lines in order to maximize energy transfer within the network system and upgrade network wide performance. NR is constantly looking for the best network parameters to save operational cost, decrease transmission loss, and increase energy efficiency [5]. In recent studies, guided by the need of dealing with the much more complex issues associated to NR algorithms, optimization techniques have been introduced in order to find optimal reconfigurations that make power flow as directionless and smooth as possible [6], [7]. However, despite the enormous potential of renewable generation, on-grid integration of these sources is difficult because they are inherently uncertain [8]. This unpredictability makes it difficult to maintain

the stability, efficiency and reliability of the network. Particle Swarm Optimization (PSO) algorithms have demonstrated the capability to address the challenges of integrating renewable energy sources into distribution networks [9].

## LITERATURE REVIEW

Recent studies have proposed various energy management strategies for operating hybrid microgrids (MGs) integrating PV and WT systems. These studies primarily aim to analyze the cost-effectiveness, fairness in energy distribution, and data privacy aspects of battery energy storage systems (BESS) [10], [11]. As shown in Table 2, researchers in this field have focused on enhancing real-time demand response and management in off-grid systems [12], developing self-optimized intelligent control systems for hybrid renewable energy resources integration [13], suggesting effective and flexible energy management for hybrid microgrids [14], and optimizing grid-connected systems through shared energy storage and cooperative alliances. In order to reduce operational costs and reduce supply-demand instability, the modern PSO optimization algorithms are used to manage the renewable energy distributions using scenario analysis and modified power distribution systems [16]. An enhanced Walrus PSO algorithm has been proposed to significantly reduce costs and voltage fluctuations, while improving stability under various uncertainty conditions [17]. Another notable advancement involves a hybrid microgrid integration method aimed at reducing power losses and improving voltage profiles in radial distribution networks [18]. An improved PSO algorithm for integrating renewable energy sources was developed in [19]. This model enables optimal planning of PV and WT farms by incorporating multiple units and inverters. Other contributions in recent research indicated that in multiple ways the study can improve sustainability, resilience, and efficiency by improving the energy system operations and integrating hybrid renewable energy sources. An advanced PSO algorithm for distributed energy systems, combining demand information with generation sources of diverse types, has been developed by the authors in [20], and the objectives are to reduce operating costs and fluctuations in energy. Another study [21] proposed a novel optimization algorithm tailored to dynamic market conditions and distributed energy resources, aiming to maximize profits and system flexibility. While a novel grey wolf-based PSO hybrid optimization was introduced by the authors in [22], it depends on the multistage bidding strategies to enhance the performance of the smart MGs and virtual power plant profitability. Predictive models of CO2 emissions and carbon allocation systems utilizing PSO-enhanced neural networks are also part of the effort to match power grids with peak carbon targets [23]Furthermore, for multi-objective optimization problems in distributed power generation systems, a combined DE-layer deep learning model is proposed with the improved PSO algorithm considering reliability, environmental effectiveness and economic cost [24]. Thereafter, two-level optimization methods, namely PSO and MWW O (PSO)-based method have been proposed to improve power quality and cost effectiveness in hydrogen-based hybrid microgrids [25]. Recent advancements have focused significantly on uncertainty-aware methodologies and robust scheduling mechanisms. For instance, robust day-ahead microgrid scheduling under demand fatigue was explored in [26], while blockchain-based peer microgrid auctions with integrated battery control were implemented under uncertainty in [27]. Intraday market participation with predictive uncertainty control was developed for residential buildings in [28], and resilient mobile storage strategies were proposed for uncertain grid environments in [29]. Self-supervised learning and ensemble methods were applied to steam flow forecasting under uncertainty in [30], while multi-microgrid scheduling incorporating mobile fuel cell storage and hybrid stochastic-robust frameworks were proposed in [31]. Hierarchical multi-agent EV control systems were enhanced using uncertainty-aware critic models in [32]. Study [33] explored demand response strategies based on deep learning for short-term optimization in renewable microgrids. Other works targeted uncertainty-aware mobile edge computing, capacitor and DSTATCOM placement using novel optimizers in distribution networks [35], and multi-agent reinforcement learning for active voltage control [36]. Furthermore, efforts toward carbon-cost dispatch and integrated energy systems were studied in [37], and data-driven energy sharing among microgrids was emphasized in [38]. Scheduling of multi-use battery storage systems with uncertainty models was addressed in [39]. Multi-energy hubs with emission and uncertainty considerations have been tackled in [40], and harmonic reduction and uncertainty mitigation via soft open point allocation are proposed in [41], and harmonic reduction and uncertainty mitigation via soft open point allocation was proposed in [42]. Transformer-based uncertainty-aware models for peer energy trading are explored in [43], and robust energy management

of microgrids under uncertainty-aware deep reinforcement learning is proposed in [44]. Finally, the inclusion of reactive power from VRE and ESS under uncertainty was formulated into optimal smart distribution frameworks in [45] (Table 2).

Table 2. Comparison of relevant literature

| Ref. | Optimal scheduling | Network constraints of DNs | Reconfiguration | Uncertainty | Switching cost allocation |
|---|---|---|---|---|---|
| [16] | √ | √ | √ | √ | × |
| [17] | √ | √ | √ | × | × |
| [18] | √ | √ | × | × | × |
| [19] | √ | × | × | √ | × |
| [20] | √ | √ | × | × | × |
| [21] | √ | × | × | × | × |
| [22] | √ | × | × | × | × |
| [23] | √ | √ | √ | × | × |
| [24] | √ | √ | × | × | × |
| [25] | √ | √ | √ | √ | × |
| [26] | √ | √ | √ | √ | × |
| [27] | √ | × | × | √ | × |
| [28] | √ | × | × | √ | × |
| [29] | √ | √ | × | √ | × |
| [30] | √ | × | × | √ | × |
| [31] | √ | √ | × | √ | × |
| [32] | √ | × | × | √ | × |
| [33] | √ | × | × | √ | × |
| [34] | √ | × | × | √ | × |
| [35] | √ | √ | × | √ | × |
| [36] | √ | √ | × | √ | × |
| [37] | √ | × | × | √ | × |
| [38] | √ | √ | × | √ | × |
| [39] | √ | × | × | √ | × |
| [40] | √ | × | × | √ | × |
| [41] | √ | √ | × | √ | × |
| [42] | √ | √ | × | √ | × |
| [43] | √ | × | × | √ | × |
| [44] | √ | √ | × | √ | × |
| [45] | √ | √ | × | √ | × |
| This paper | √ | √ | √ | √ | √ |

**Research Gap**

Current studies in the literature exhibit several key limitations.

- A notable gap exists in implementing globally distributed trading mechanisms that inclusively involve all participants, despite the growing emphasis on privacy in multi-microgrid (MMG) energy trading.

- Furthermore, while robust optimization effectively manages uncertainty, its reliance on worst-case scenarios often leads to overly conservative decisions that may not reflect practical operational efficiencies in real-world conditions.

- The modeling challenges in MMGs are not thoroughly investigated, specifically with the dual concern of uncertainty and proper switching cost allocation together.

- Lack of physical network constraints: The majority of the trading models with quantity flexibility assume an ideal model which usually do not take into DNs' fundamental physical network constraint, leading to unrealistic scheduling results and eventually flow-based market participation autonomy of Mgs. This omission demonstrates the continuing requirement for integrated methods, such as reconfiguration techniques, in order to enforce physical network constraints on energy trading.

**Contribution**

There are several novel contributions of this study to the literature of decentralized energy management and power distribution network optimization. The contribution of this paper can be summarized as follows:

- A customized PSO to optimize the electric distribution performance in the MGD system.

- Three-scenario analysis: Working in TPC network to quantitatively examine the effect of PSO and network reconfiguration. (1) C 1: Baseline scenario (TPC operation and without renewable, PSO, network reconfiguration). (2) Configuration 2: to model the TPC operation with renewables, and PSO, without any reconfiguration. (3) Case 3: the TPC transmission using renewables, PSO and network reconfiguration.

**Paper Layout**

The remainder of this paper is structured as follows: Section 2 presents the proposed methodology, including system modeling, the uncertainty-aware PSO algorithm, and a representation of the IEEE 84-bus TPC network. Section 3 outlines the multi-scenario simulation framework used to evaluate three operational configurations. Section 4 describes the simulation results, comparing performance across power loss, voltage stability, and cost. Section 5 discusses the findings and section 6 concludes the implications of the findings and the robustness of the proposed strategy by summarizing key contributions and future directions.

## MODELING AND FORMULATION

The cost effectiveness of energy trading in a smart grid is maximized while total operational costs are minimized via the objective function. This is obtained by the optimization of two terms: Total operational costs sum among all participating microgrids, and Penalty term which both quantifies and compensates for the risk incorporated with uncertainty of power generation from renewable sources. Through such an explicit reduction of renewable energy fluctuation variance, the optimization framework further improves economic efficiency and system robustness against unpredictable power outputs arising from renewables. This multi-prong approach is designed to manicure that the energy trading decisions made are low cost and robust to fluctuations in renewable-based sources of power, such as solar and wind.

The objective function to be minimized can be formulated as follows equation 1 and 2:

$$min\ \left(\sum_{i=1}^{N} C_i(x_i) + \lambda \cdot Var(\Delta P_{RE})\right) \quad (1)$$

Variations in wind and solar energy are modeled as stochastic deviations from their expected values.

$$P_{RE} = \overline{P}_{RE} + \Delta P_{RE} \quad (2)$$

*Adding renewable energy to MMG*

The power output from a solar PV system, $P_{PV}$, is calculated by equation 3:

$$P_{PV}=\eta_{PV}\cdot A\cdot G\cdot \cos(\theta) \quad (3)$$

The power output of a wind turbine, $P_{Wind}$, is expressed as equation 4:

$$P_{Wind}=\frac{1}{2}\cdot\rho\cdot A\cdot v^3\cdot C_p \quad (4)$$

Accurate mathematical modeling of PV and WT generation units is essential for understanding the role of distributed renewable resources in the operation of microgrids and MMG systems.

*The Constraints Imposed on Reconfiguration*

The reconfiguration process is subject to a set of constraints that maintain network stability, operational efficiency, and radial topology. These constraints, formulated based on power flow equations and binary connectivity variables, are mathematically expressed as follows:

*Net Power Balance Equations*

At each node k and time t, the balance of active and reactive power is computed by considering all incoming, outgoing, curtailed, flexible, and shed power components which are shown in equation 5 and 6.

$$P_{k,t}^{net}=P_{k,t}^{b}+P_{k,t}^{L}+P_{k,t}^{L,drp}-P_{k,t}^{fc}+P_{k,t}^{el}-P_{k,t}^{L,shedded} \quad (5)$$

$$Q_{k,t}^{net}=Q_{k,t}^{L}+Q_{k,t}^{L,drp}-Q_{k,t}^{L,shedded} \quad (6)$$

*Power Flow Constraints*

The net active and reactive power at node k must lie within bounds defined by the difference between incoming and outgoing power, modified by line status variables via the Big-M formulation. It was represented by equation (7), (8), (9), (10),

$$P_{k,t}^{net}\geq P_{ik,t}-\sum_{j\in T}P_{ik,t}-\left[1-\gamma_{ik,t}\right]\cdot M \quad (7)$$

$$P_{k,t}^{net}\leq P_{ik,t}-\sum_{j\in T}P_{ik,t}+[1-\gamma_{ik,t}]\cdot M \quad (8)$$

$$Q_{k,t}^{net}\geq Q_{ik,t}-\sum_{j\in T}Q_{ik,t}-\left[1-\gamma_{ik,t}\right]\cdot M \quad (9)$$

$$Q_{k,t}^{net}\leq Q_{ik,t}-\sum_{j\in T}Q_{ik,t}+[1-\gamma_{ik,t}]\cdot M \quad (10)$$

*Voltage Constraints*

The voltage at bus *k* must be bounded by the sending-end voltage $U_{i,t}$, adjusted for line losses and conditional on the operational status of the line. Also, it is not greater than the sending voltage, factoring in power flow and status of the line using the big-M formulation are illustrated in equation (11), (12), (13).

$$U_{k,t}\geq U_{i,t}-\frac{r_{ik}P_{ik,t}+x_{ik}Q_{ik,t}}{U_{1,t}}-\left[1-\gamma_{ik,t}\right]\cdot M \quad (11)$$

$$U_{k,t} \leq U_{i,t} - \frac{r_{ik}P_{ik,t} + x_{ik}Q_{ik,t}}{U_{1,t}} + \left[1 - \gamma_{ik,t}\right] \cdot M \quad (12)$$

$$U_i^{min} \leq U_{i,t} \leq U_i^{max} \quad (13)$$

*Line Flow Constraints*

The active power flow $P_{ik,\,t}$ must remain within its allowable limits, determined by the line status $\gamma_{ik,\,t}$, which indicates whether the line is ON or OFF. Moreover, the reactive power flow $Q_{ik,\,t}$ on a line between buses *i* and *k* must be constrained within its maximum allowable range, depending on the status of the line in equation 14 and 15.

$$-\gamma_{ik,t} \cdot P_{ik}^{max} \leq P_{ik,t} \leq \gamma_{ik,t} \cdot P_{ik}^{max} \quad (14)$$

$$-\gamma_{ik,t} \cdot Q_{ik}^{max} \leq Q_{ik,t} \leq \gamma_{ik,t} \cdot Q_{ik}^{max} \quad (15)$$

*Radial Operation Constraints:*

The spanning tree approach enforces directionality symmetry, ensuring that connections between nodes *i to k* and *k to i* align with the binary line status $\gamma_{ik,\,t}$ are shown in equation 16.

$$\beta_{ik,t} + \beta_{ki,t} = \gamma_{ik,t} \quad (16)$$

Root node constraint specifies that the root bus (node 0) does not have any incoming branches, forming the starting point of the radial topology in equation 17.

$$\sum_k \beta_{k0,t} = 0 \quad (17)$$

The tree branch constraint limits each node to a maximum of one incoming edge, thereby preserving a loop-free radial structure in equation 18.

$$\sum_k \beta_{ki,t} \leq 1 \quad (18)$$

*Power Flow Analysis*

For a system of nonlinear equations f(x)=0, the Newton-Raphson iterative update is given by equation 19,

$$x^{(k+1)} = x^{(k)} - J^{-1}(x^{(k)}) \cdot f(x^{(k)}) \quad (19)$$

In MMGs, the power flow problem requires solving nonlinear equations 20 and 21 that represent the balance of active (P) and reactive (Q) power at each bus.

$$P_i = V_i \sum_{j-1}^{N} V_j \left(G_{ij}\ cos\,\theta_{ij} + B_{ij}\ sin\,\theta_{ij}\right) \quad (20)$$

$$Q_i = V_i \sum_{j-1}^{N} V_j \left(G_{ij}\ sin\,\theta_{ij} - B_{ij}\ cos\,\theta_{ij}\ \right) \quad (21)$$

*Application of the optimization techniques for MMG (PSO optimization technique)*

The fitness function is adapted to account for uncertainty are represented by equation 22:

$$Fitness(x) = w \cdot Cost(x) + (1-w) \cdot Resilience(x) \quad (22)$$

In the PSO-based optimization framework for MMGs, the fitness function is designed to incorporate

uncertainty by combining two objectives: minimizing cost and maximizing resilience. Each particle updates its position by adding its velocity to its current location at every iteration. This dynamic movement enables a broad exploration of the solution space. Each particle adjusts its trajectory based on its personal best position and the global best position found by the swarm. The location update equation 23 explains this as follows:

$$x_i^{(t+1)}=x_i^{(t)}+v_i^{(t+1)} \tag{23}$$

In PSO, each particle's velocity is influenced by three components: inertia (tendency to maintain current direction), cognitive influence (attraction toward its own best-known position), and social influence (attraction toward the swarm's global best position). These influences are combined within an equation 24 to update the particle's velocity

$$v_i^{(t+1)}=w\cdot v_i^{(t)}+c_1\cdot r_1\cdot\left(p_i^{best}-x_i^{(t)}\right)+c_2\cdot r_2\cdot\left(g^{best}-x_i^{(t)}\right) \tag{24}$$

The inertia weight (w) balances exploration (global search) and exploitation (local refinement), which is essential for achieving convergence in PSO.

**Cost Equations and Their Integration into Optimization Functions**

Efficient electricity trading requires minimizing the overall operational cost of the distribution network to ensure balanced supply and demand. The total cost in a microgrid typically includes three components: generation cost, trading cost (buying/selling electricity), and penalty cost incurred when electricity demand is unsupplied. The electricity generation cost is modeled as followed equation 25:

$$C_{i,t}^{Gen}=\lambda_i^{MT}p_{i,t}^{MT}+\lambda_i^{BS}p_{i,t}^{BSC}+p_{i,t}^{BSD}+k_i^{TS}\left(H_{i,t}^{TSC}+H_{i,t}^{TSD}\right) \tag{25}$$

PROPOSED FRAMEWORK

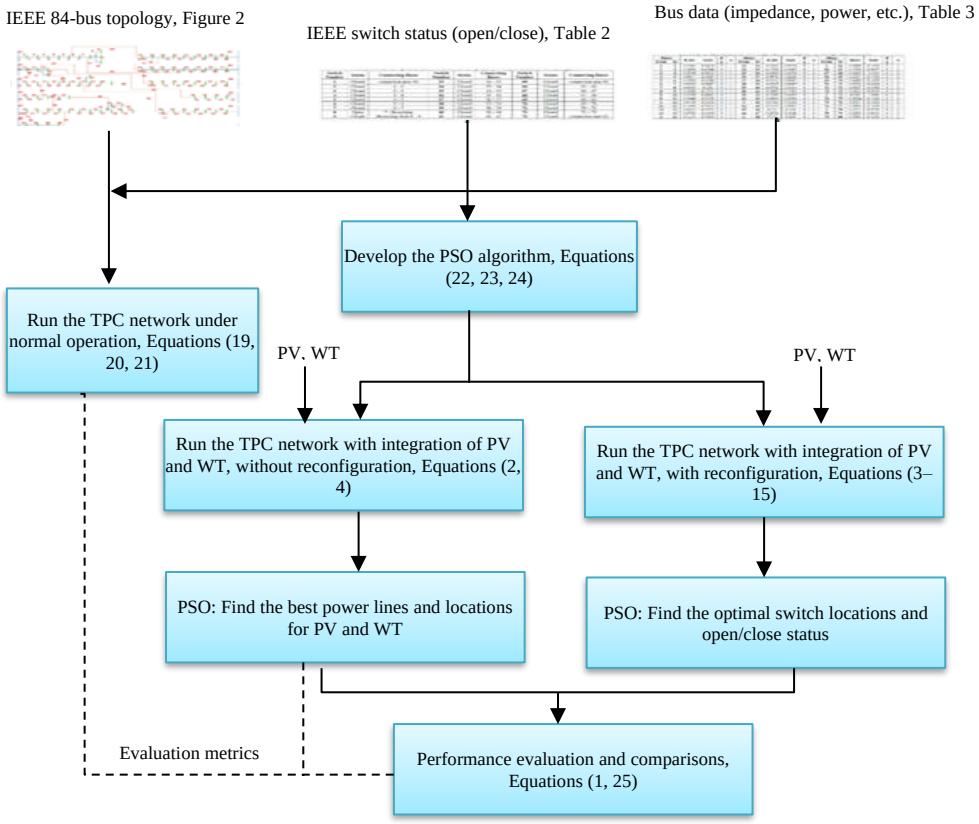


Figure 1. Flowchart of the proposed framework for PV and WT integration and reconfiguration in the TPC system

A multi-scenario configuration methodology is proposed in Fig. 1), supported by a simulation-based study to evaluate hybrid renewable energy integration and dynamic network reconfiguration in the TPC distribution system. The PSO algorithm is employed to enable decentralized, stable, and flexible integration of wind turbines and renewable energy sources [34]. Figure 1 illustrates a multi-phase methodology, comprising data preprocessing, initial system setup, and performance evaluation as its core phases.

**The IEEE 84-bus for the TPC**

TPC has a large and technically complex transmission-distribution grid covering the entire island of Taiwan. That is why the study have such a strong infrastructure enabling us to trade energy with precision and transmit power quickly and efficiently across our entire region. This paper proposes a new representation of the IEEE 84-bus layout for the TPC network shown in Figure 2. In a preferred embodiment, the topology depicts reconfigure nodes and transmission line infrastructure.

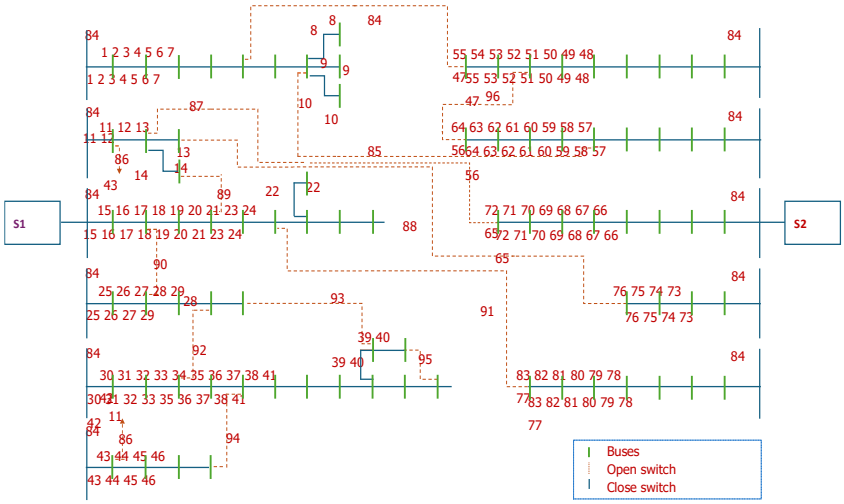


Figure 2. Schematic of the IEEE 84-bus distribution

The IEEE 84-bus network will be used as the backbone of our analysis, offering good readings to investigate MG reconfiguration optimization algorithms and decentralized energy trading [15]. A systematic operational condition of each switch and a property of connecting line are shown in Table 3. The network map consists of two primary supply sources (S1/MicroGrid_1 and S2/MicroGrid_2), a system of interconnected buses along with controllable switches. Switches in the ON condition are controlled by solid green lines (closed) and dashed orange lines (open), representing active or isolated paths, respectively. In the present setting, the radial-shaped segmentation is observed in which S1 provides for the lower-left and central left regions while S2 provides for the upper-right and lower right regions. Importantly, the large number of open (tie) switches represents an important network reconfiguration possibility and allows a more efficient operation for different purposes, including load factor improvement load factor correction, fault isolation voltage profile improvement power loss reduction distributed generation (PV and WT) optimal integration.

**Algorithm 1: Hybrid Solar-Wind Integration Using PSO**

Input:

- IEEE 84-bus network model
- Initial power injection data $P_i^{(0)}$ for each bus $i$
- Renewable energy (PV, WT) with output power $P_{PV}, P_{WT}$
- PSO parameters: swarm size $N$, iterations $T$, and coefficients $c_1, c_2, w$

Output:

- Optimized network configuration: {$P_{PV}$, $P_{WT}$, switch positions}
- Performance metrics: cost, losses, voltage stability

Step 1: Initialize Network

Let the network model $G$be represented as:

- $G = (V, E)$, where $V$is the set of nodes (buses) and $E$is the set of edges (connections).
- Initial power and impedance data are provided for each line:

$Z_{ij} = R_{ij} + jX_{ij}$for each line (i, j)Step 2: Initialize PSO

For each particle $p$in the swarm, initialize the following:

- Position: $X_p^{(0)} = \{P_{PV}, P_{WT},$switch locations$\}$
- Velocity: $V_p^{(0)}$
- Fitness: $f_p^{(0)} =$ Cost Function$(X_p^{(0)})$

Where:

$f_p = C_{\text{generation}}(P_{PV}, P_{WT}) + C_{\text{losses}}(P_i)$Step 3: Fitness Calculation

For each particle $p$, calculate the fitness:

$f_p = C_{\text{generation}}(P_{PV}, P_{WT}) + C_{\text{losses}}(P_i)$Subject to the following constraints:

- Voltage constraints at bus $k$:

$V_k^{\min} \le V_k \le V_k^{\max}$Power flow constraints between buses $i$and $k$:

$$P_{ik} = \frac{V_i V_k}{Z_{ik}} \text{ for active power} Q_{ik} = \frac{V_i V_k}{Z_{ik}} \text{ for reactive power}$$

Step 4: Update PSO

Update the position and velocity of each particle using:

$$V_p^{(t+1)} = wV_p^{(t)} + c_1 r_1 (X_p^{\text{best}} - X_p^{(t)}) + c_2 r_2 (X_{\text{global}}^{\text{best}} - X_p^{(t)})$$

Update the position:

$X_p^{(t+1)} = X_p^{(t)} + V_p^{(t+1)}$Step 5: Evaluate Performance

For each updated position $X_p^{(t+1)}$:

- Run the power flow calculation to find $P_i, Q_i$for each bus.
- Calculate performance metrics like:

Total Cost $= \sum_i (C_{\text{generation}}(P_i) + C_{\text{losses}}(P_i))$Voltage Stability Metric $= \sum_i (V_i - V_{\text{nominal}})^2$ Step 6: Check Convergence

Check for convergence by comparing the change in the best cost function value:

$$\Delta f_{\text{best}} = | f_{\text{best}}^{(t)} - f_{\text{best}}^{(t-1)} |$$

If $\Delta f_{\text{best}} < \epsilon$(a small threshold), then stop.

Step 7: Output Results

Return the optimized configurations:

- $\{P_{PV}, P_{WT},$ switch locations$\}$
- Performance metrics: {cost, losses, voltage stability}

A smart grid with hybrid solar-wind integration can be optimized with the help of Particle Swarm Optimization (PSO) as presented in Algorithm 1. This starts with initializations of the IEEE 84-bus network and PSO parameters then calculates the fitness of each particle against the generation costs and the power losses. The algorithm restarts the procedure of redefining the location of the particles and their velocity, measures of effectiveness, including cost and voltage steadiness, and convergent tests. Once convergence occurs, the best network configuration and performance condition is replicated (Table 3).

Table 3. Status of switches in the IEEE 84-bus distribution network under normal operating conditions

| Switch Number | Status | Connecting Buses | Switch Number | Status | Connecting Buses | Switch Number | Status | Connecting Buses |
|---|---|---|---|---|---|---|---|---|
| 1 | Closed | connection near S1 | 33 | Closed | 32 – 33 | 65 | Closed | connection near S2 |
| 2 | Closed | 1 – 2 | 34 | Closed | 33 – 34 | 66 | Closed | 65 – 66 |
| 3 | Closed | 2 – 3 | 35 | Closed | 34 – 35 | 67 | Closed | 66 – 67 |
| 4 | Closed | 3 – 4 | 36 | Closed | 35 – 36 | 68 | Closed | 67 – 68 |
| 5 | Closed | 4 – 5 | 37 | Closed | 36 – 37 | 69 | Closed | 68 – 69 |
| 6 | Closed | 5 – 6 | 38 | Closed | 37 – 38 | 70 | Closed | 69 – 70 |
| 7 | Closed | 6 – 7 | 39 | Closed | 38 – 39 | 71 | Closed | 70 – 71 |
| 8 | Open | 7 - Branching | 40 | Closed | 39 – 40 | 72 | Closed | 71 – 72 |
| 9 | Closed | Branching from 8 – 9 | 41 | Closed | 40 – 41 | 73 | Closed | connection near S2 |
| 10 | Open | 9 - Branching | 42 | Closed | 41 – 42 | 74 | Closed | 73 – 74 |
| 11 | Closed | connection near S1 | 43 | Closed | near S1 | 75 | Closed | 74 – 75 |
| 12 | Closed | 11 – 12 | 44 | Closed | 43 – 44 | 76 | Closed | 75 – 76 |
| 13 | Open | 12 - Branching | 45 | Closed | 44 – 45 | 77 | Closed | 76 – 77 |
| 14 | Open | Branching from 13 | 46 | Closed | 45 – 46 | 78 | Closed | 77 – 78 |
| 15 | Closed | connection near S1 | 47 | Closed | near S2 | 79 | Closed | 78 – 79 |
| 16 | Closed | 15 – 16 | 48 | Closed | 47 – 48 | 80 | Closed | 79 – 80 |
| 17 | Closed | 16 – 17 | 49 | Closed | 48 – 49 | 81 | Closed | 80 – 81 |
| 18 | Closed | 17 – 18 | 50 | Closed | 49 – 50 | 82 | Closed | 81 – 82 |
| 19 | Closed | 18 – 19 | 51 | Closed | 50 – 51 | 83 | Closed | 82 – 83 |
| 20 | Closed | 19 – 20 | 52 | Closed | 51 – 52 | 84 | Open | Multiple branching |
| 21 | Closed | 20 – 21 | 53 | Closed | 52 – 53 | 85 | Open | Reconfiguration |
| 22 | Open | 21 - Branching | 54 | Closed | 53 – 54 | 86 | Open | Reconfiguration |
| 23 | Closed | Branching from 22 – 23 | 55 | Closed | 54 – 55 | 87 | Open | Reconfiguration |
| 24 | Closed | 23 – 24 | 56 | Closed | near S2 | 88 | Open | Reconfiguration |
| 25 | Closed | connection near S1 | 57 | Closed | 56 – 57 | 89 | Open | Reconfiguration |
| 26 | Closed | 25 – 26 | 58 | Closed | 57 – 58 | 90 | Open | Reconfiguration |
| 27 | Closed | 26 – 27 | 59 | Closed | 58 – 59 | 91 | Open | Reconfiguration |
| 28 | Closed | 27 – 28 | 60 | Closed | 59 – 60 | 92 | Open | Reconfiguration |
| 29 | Closed | 28 – 29 | 61 | Closed | 60 – 61 | 93 | Open | Reconfiguration |
| 30 | Closed | connection near S1 | 62 | Closed | 61 – 62 | 94 | Open | Reconfiguration |
| 31 | Closed | 30 – 31 | 63 | Closed | 62 – 63 | 95 | Open | Reconfiguration |
| 32 | Closed | 31 – 32 | 64 | Closed | 63 – 64 | 96 | Open | Reconfiguration |

A set of basic input values such as line impedances, initial equilibrium power injections and open circuit paths are inputs to the simulation scheme that allows the computation of derived parameters and

measurements adjustable under optimal load flow. Line impedance has an important influence on power flow optimization and loss calculation. Tables 4 and 5 systematically summarize tabulations for the input power parameters and impedance characteristics, respectively. In particular, Table 4 presents network topology and provides actual values of resistance (R), reactance (X), half-shunt susceptance (B/2) and transformer tap ratio (a) for each line segment in the transmission. These specific results are very useful for network modeling and power flow convergence. They are valuable resources for the realization of advanced power system strategies, such as load restoration, fault isolation and alternate path to provide that make it possible to have an intentional control over the pattern of power flow and also lead to a more resilient network.

Table 4. Characteristics of transmission lines in the distribution TPC network. the table details the resistance (r), reactance (x), half of the shunt susceptance (b/2), and transformer tap ratio (a)

| Buses | | R (Ω) | X(Ω) | $\frac{B}{2}$ | A | Buses | | R (Ω) | X(Ω) | $\frac{B}{2}$ | A | Buses | | Buses | X(Ω) | $\frac{B}{2}$ | A |
|---|---|---|---|---|---|---|---|---|---|---|---|---|---|---|---|---|---|
| From | To | | | | | From | To | | | | | From | To | | | | |
| 1 | 2 | 0.1944 | 0.6624 | 0 | 1 | 33 | 34 | 0.0262 | 0.0538 | 0 | 1 | 1 | 66 | 0.0486 | 0.1656 | 0 | 1 |
| 2 | 3 | 0.2096 | 0.4304 | 0 | 1 | 34 | 35 | 0.1703 | 0.3497 | 0 | 1 | 66 | 67 | 0.1703 | 0.3497 | 0 | 1 |
| 3 | 4 | 0.2358 | 0.4842 | 0 | 1 | 35 | 36 | 0.0524 | 0.1076 | 0 | 1 | 67 | 68 | 0.1215 | 0.414 | 0 | 1 |
| 4 | 5 | 0.0917 | 0.1883 | 0 | 1 | 36 | 37 | 0.4978 | 1.0222 | 0 | 1 | 68 | 69 | 0.2187 | 0.7452 | 0 | 1 |
| 5 | 6 | 0.2096 | 0.4304 | 0 | 1 | 37 | 38 | 0.0393 | 0.0807 | 0 | 1 | 69 | 70 | 0.0486 | 0.1656 | 0 | 1 |
| 6 | 7 | 0.0393 | 0.0807 | 0 | 1 | 38 | 39 | 0.0393 | 0.0807 | 0 | 1 | 70 | 71 | 0.0729 | 0.2484 | 0 | 1 |
| 7 | 8 | 0.0405 | 0.138 | 0 | 1 | 39 | 40 | 0.0786 | 0.1614 | 0 | 1 | 71 | 72 | 0.0567 | 0.1932 | 0 | 1 |
| 8 | 9 | 0.1048 | 0.2152 | 0 | 1 | 40 | 41 | 0.2096 | 0.4304 | 0 | 1 | 72 | 73 | 0.0262 | 0.0528 | 0 | 1 |
| 8 | 10 | 0.2358 | 0.4842 | 0 | 1 | 39 | 42 | 0.1965 | 0.4035 | 0 | 1 | 1 | 74 | 0.324 | 1.104 | 0 | 1 |
| 8 | 11 | 0.1048 | 0.2152 | 0 | 1 | 42 | 43 | 0.2096 | 0.4304 | 0 | 1 | 74 | 75 | 0.0324 | 0.1104 | 0 | 1 |
| 1 | 12 | 0.0786 | 0.1614 | 0 | 1 | 1 | 44 | 0.0486 | 0.1656 | 0 | 1 | 75 | 76 | 0.0567 | 0.1932 | 0 | 1 |
| 12 | 13 | 0.3406 | 0.6944 | 0 | 1 | 44 | 45 | 0.0393 | 0.0807 | 0 | 1 | 76 | 77 | 0.0486 | 0.1656 | 0 | 1 |
| 13 | 14 | 0.0262 | 0.0538 | 0 | 1 | 45 | 46 | 0.131 | 0.269 | 0 | 1 | 1 | 78 | 0.2511 | 0.8556 | 0 | 1 |
| 13 | 15 | 0.0786 | 0.1614 | 0 | 1 | 46 | 47 | 0.2358 | 0.4842 | 0 | 1 | 78 | 79 | 0.1296 | 0.4416 | 0 | 1 |
| 1 | 16 | 0.1134 | 0.3864 | 0 | 1 | 1 | 48 | 0.243 | 0.828 | 0 | 1 | 79 | 80 | 0.0486 | 0.1656 | 0 | 1 |
| 16 | 17 | 0.0524 | 0.1076 | 0 | 1 | 48 | 49 | 0.0655 | 0.1345 | 0 | 1 | 80 | 81 | 0.131 | 0.264 | 0 | 1 |
| 17 | 18 | 0.0524 | 0.1076 | 0 | 1 | 49 | 50 | 0.0655 | 0.1345 | 0 | 1 | 81 | 82 | 0.131 | 0.264 | 0 | 1 |
| 18 | 19 | 0.1572 | 0.3228 | 0 | 1 | 50 | 51 | 0.0393 | 0.0807 | 0 | 1 | 82 | 83 | 0.0917 | 0.1883 | 0 | 1 |
| 19 | 20 | 0.0393 | 0.0807 | 0 | 1 | 51 | 52 | 0.0786 | 0.1614 | 0 | 1 | 83 | 84 | 0.3144 | 0.6456 | 0 | 1 |
| 20 | 21 | 0.1703 | 0.3497 | 0 | 1 | 52 | 53 | 0.0393 | 0.0807 | 0 | 1 | 6 | 56 | 0.131 | 0.269 | 0 | 1 |
| 21 | 22 | 0.2358 | 0.4842 | 0 | 1 | 53 | 54 | 0.0786 | 0.1614 | 0 | 1 | 8 | 61 | 0.131 | 0.269 | 0 | 1 |
| 22 | 23 | 0.1572 | 0.3228 | 0 | 1 | 54 | 55 | 0.0524 | 0.1076 | 0 | 1 | 12 | 44 | 0.131 | 0.269 | 0 | 1 |
| 22 | 24 | 0.1965 | 0.4035 | 0 | 1 | 55 | 56 | 0.131 | 0.269 | 0 | 1 | 13 | 73 | 0.3406 | 0.6994 | 0 | 1 |
| 24 | 25 | 0.131 | 0.269 | 0 | 1 | 1 | 57 | 0.2268 | 0.7728 | 0 | 1 | 14 | 77 | 0.4585 | 0.9415 | 0 | 1 |
| 1 | 26 | 0.0567 | 0.1932 | 0 | 1 | 57 | 58 | 0.5371 | 1.1029 | 0 | 1 | 15 | 19 | 0.5371 | 1.0824 | 0 | 1 |
| 26 | 27 | 0.1048 | 0.2152 | 0 | 1 | 58 | 59 | 0.0524 | 0.1076 | 0 | 1 | 17 | 27 | 0.0917 | 0.1883 | 0 | 1 |
| 27 | 28 | 0.2489 | 0.5111 | 0 | 1 | 59 | 60 | 0.0405 | 0.138 | 0 | 1 | 21 | 84 | 0.0786 | 0.1614 | 0 | 1 |
| 28 | 29 | 0.0486 | 0.1656 | 0 | 1 | 60 | 61 | 0.0393 | 0.0807 | 0 | 1 | 29 | 33 | 0.0524 | 0.1076 | 0 | 1 |
| 29 | 30 | 0.131 | 0.269 | 0 | 1 | 61 | 62 | 0.0262 | 0.0538 | 0 | 1 | 30 | 40 | 0.0786 | 0.1614 | 0 | 1 |
| 1 | 31 | 0.1965 | 0.396 | 0 | 1 | 62 | 63 | 0.1048 | 0.2152 | 0 | 1 | 35 | 47 | 0.0262 | 0.0538 | 0 | 1 |
| 31 | 32 | 0.131 | 0.269 | 0 | 1 | 63 | 64 | 0.2358 | 0.4842 | 0 | 1 | 41 | 43 | 0.1965 | 0.4035 | 0 | 1 |
| 32 | 33 | 0.131 | 0.269 | 0 | 1 | 64 | 65 | 0.0243 | 0.0828 | 0 | 1 | 54 | 65 | 0.0393 | 0.0807 | 0 | 1 |

Table 5. Initial injected power for transmission lines

| Index | Injection Power (Mw) | Index | Injection Power (Mw) |
|---|---|---|---|
| 1 | 488.712139517526 | 13 | 1200 |
| 2 | 1200 | 14 | 0 |
| 3 | 1200 | 15 | 1166.23993372747 |
| 4 | 117.344788762350 | 16 | 1200 |
| 5 | 122.066192223495 | 17 | 1200 |
| 6 | 1019.65073498411 | 18 | 1200 |
| 7 | 1124.81406364160 | 19 | 1200 |
| 8 | 777.261295231962 | 20 | 1200 |
| 9 | 1184.07666584809 | 21 | 1200 |
| 10 | 140.748290651205 | 22 | 1200 |
| 11 | 1200 | 23 | 0 |
| 12 | 1035.28296513910 | 24 | 1200 |

**Multi-configuration scenarios**

The proceeding data processing describes how the simulation environment is built, and how data obtained by analyzing TPC work are processed. This stage explicitly deals with the uncertainties caused by renewable energy penetration, and their influences on trading behaviors among MGs. Various characteristics are examined within the base case study of TPC, in which traditional methodology to find feasible placement of switches is employed for better energy distribution, and power flow enhancement without considering renewable energy. Then, the study is developed in steps: considering PV and WT generation combined with PSO-based optimal switch allocation without reconfiguration to combat cost uncertainty / voltage drop; and then including reconfiguration (with PSO) for optimally placing/positioning switches for combining switches/PV power with core objective of loss reduction given optimal cost.

*Configuration 1:*

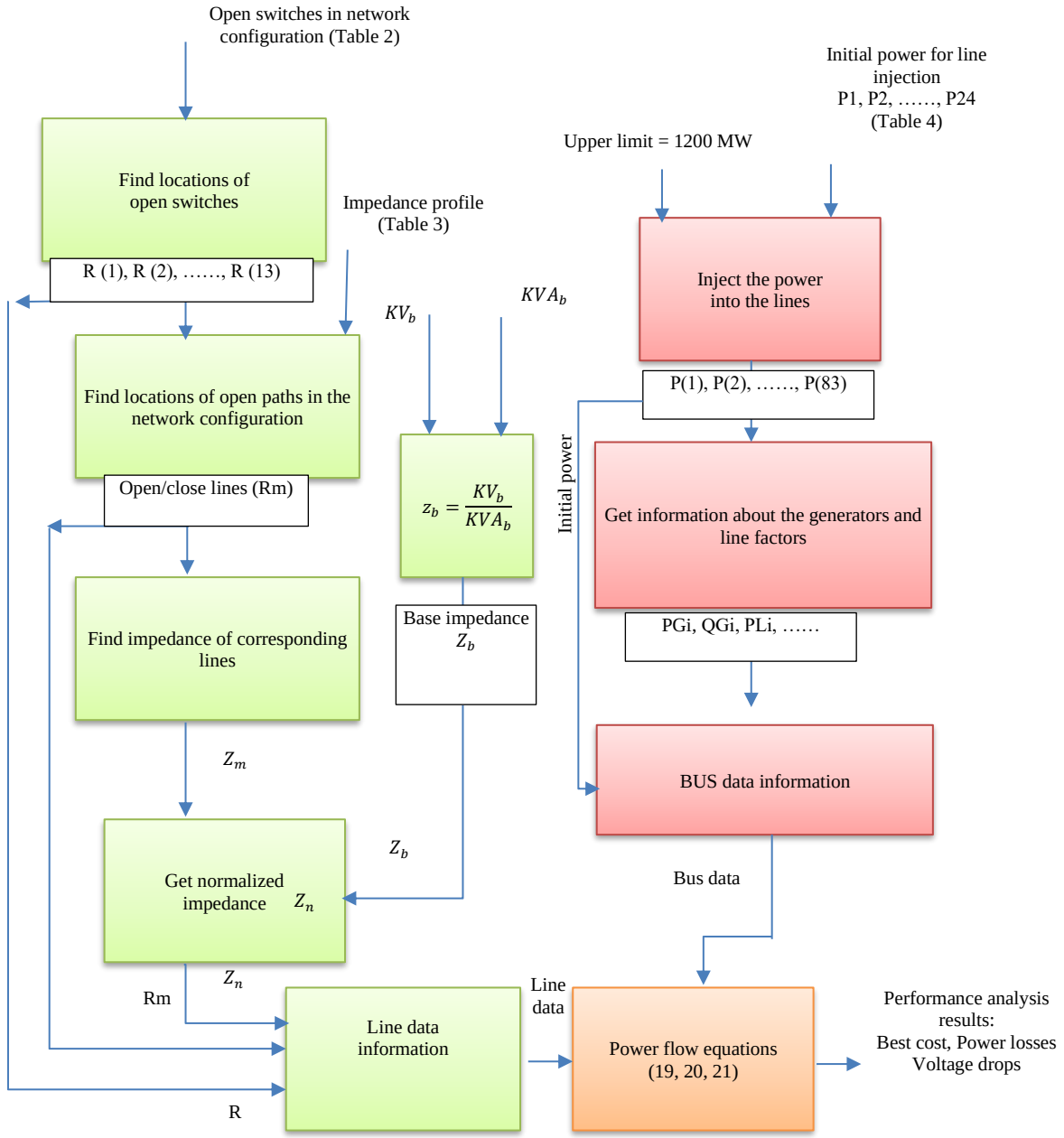


Figure 3. Operational sequence of the TPC power network distribution simulation

The simulation of the TPC power network, shown in Figure 3, is developed based on critical inputs such as the status of switches (Table 3), line impedance data (Table 4), and size of initial power injections (Table 5). This information allows a formulation of a mathematical model for an optimal choice of switches and line parameters, as well as the resulting power flow algorithm. Starting out with acquisition of input data the process also contains determination of network topology; open/closed switches and lines, retrieval for line impedance values (104). For uniformity in the power flow calculations, line impedances are transformed to per-unit (p.u.). Comprehensive line and system state initialization data are then formed that include power injection, generation, and load information. Central to this is the Newton-Raphson approach to solving power flow equations (Equations 19--21), from which important performance indices, namely, optimal cost, power losses and voltage drop are obtained. These findings provide important feedback about the effectiveness, availability and performance of the TPC network in its normal operation.

*Configuration 2 and 3:*

The following sub-sections describe the process of applying the PSO algorithm shown in Figure 4 over several stages to obtain the best configuration of the system and its operation conditions. The main goal is to minimize the power costs and losses in the network for different RES integration possibilities. Initially, the PSO process was initiated by accurately setting the problem parameters, such as; number of decision variables involved, their range (lower and upper limit) searching spaces and an initial cost function, based on a reference power network injection for IEEE 84-bus system. At the same time, parameters of PSO that are specific to this method such as swarm size or maximum iterations along with initial inertia weight mingled with their damping ratio and cognitive/social learning coefficients are appropriately tuned in order to control its well-balanced explorative/explotative searching trend. In the initialization, each particle is placed in a random position with zero velocity (initial personal and global best) solutions. The basic optimization is conducted in an iterative manner, where the velocities are calculated from each particle's personal/PBest and GBest corrections as well as blueprinted via (22, 23, 24) and finally treated for constraints whereby the particles' positions are subsequently updated. During each iteration, all the computed neighbor positions are analyzed and the local best and global best solutions are further optimized by a single particle based on weight inertia reducing metric. At convergence, the algorithm provides the optimal cost (bestCost), its trajectory, and the corresponding optimal values for power injections and line parameters (including that of switch positions) for use in further power flow computations, system placement analysis as well as permitting network reconfiguration strategies designed to improve system operation.

The integration of both PV and WT systems extends the baseline methodology described in Equations (3) and (4). The addition of PV and WT systems makes the optimization problem much more complex and dimensional, and a more comprehensive approach must be adopted, even if the overall grid structure and PSO framework do not change. At this point in the methodology, the simulation analysis is extended and moved towards grid optimization by introducing the concept of grid reconfiguration. By exploiting the functionality of the PSO algorithm, switching points are wisely reconfigured to build a new optimized topology of the network.

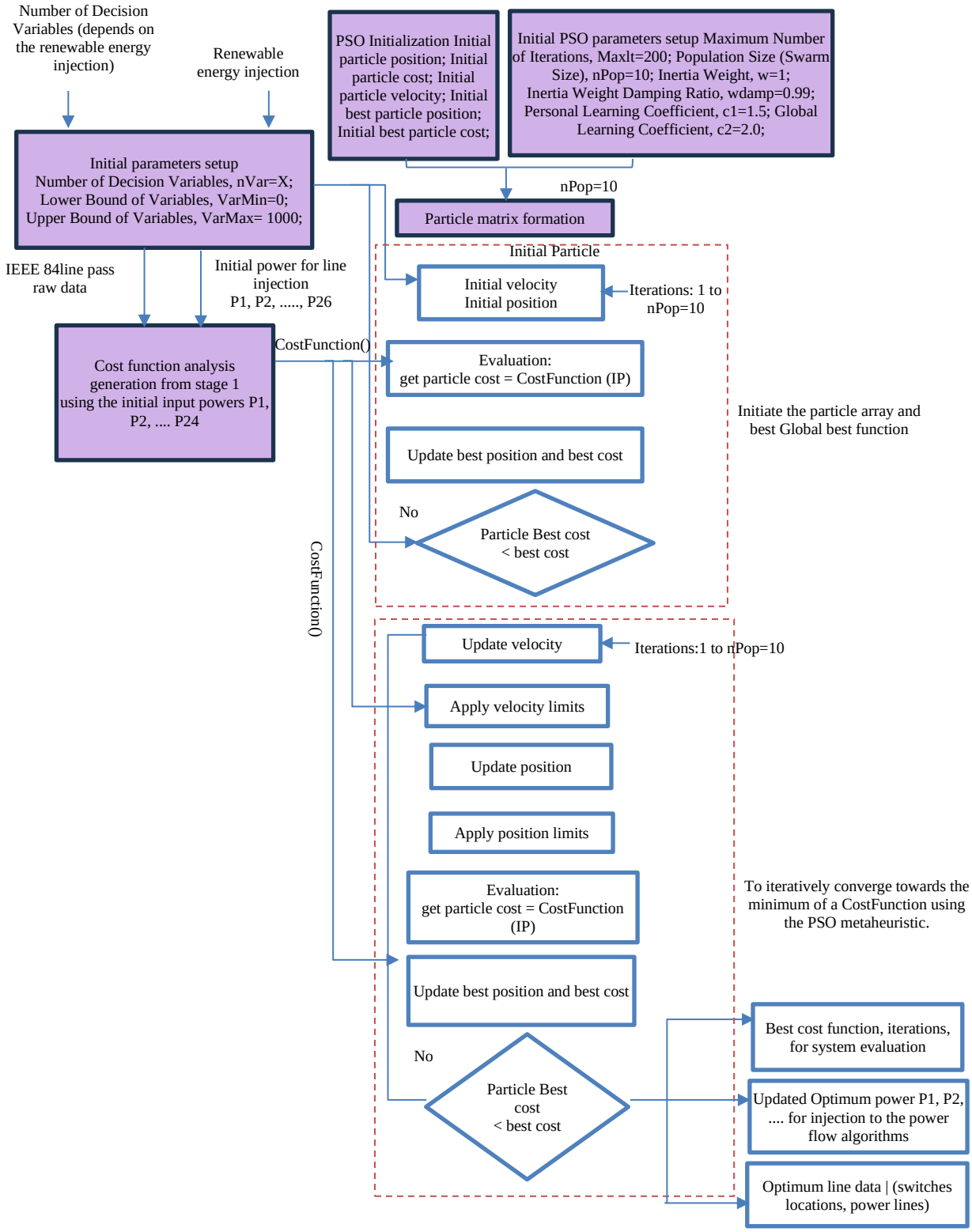


Figure 4. Detailed flowchart of the PSO algorithm

THE PERFORMANCE EVALUATION

The simulation results that are obtained during the data preprocessing phase are carefully and thoroughly analyzed during the performance evaluation phase. This phase starts with a full evaluation of important system performance metrics. In addition to specific best-cost metrics, such as operating cost and installation efficiency calculated from the initial unoptimized network architecture (Equation 25), this includes such metrics as voltage deviations from nominal values and total active and passive power losses.

This first evaluation serves as a crucial standard by which to measure any further advancements. To measure efficiency and usefulness in practical application, a comparative analysis is performed on different cases of network reconfiguration with PSO optimization, including the detailed analysis of the PSO performance (convergence rate, number of iterations, and parameter sensitivity). In order to explicitly demonstrate the observable benefits in terms of operational efficiency and stability of the system, one of the main components of this stage is direct and quantitative comparison of critical metrics in terms of (mostly) power losses and voltage profiles of the original and PSO-optimized reconfigured topologies, especially for integrated PV and WT generation scenarios. In order to understand the significance of observed changes, the results of all the simulated scenarios are then extensively compared with sophisticated statistical analysis and data visualisation methods. The major goal is to provide accurate fact-based results on the efficacy of PSO-based operating network reconfiguration for the integration of RES and effective energy trading on TPC distribution network to promote the smart grid technologies and sustainable energy practices.

**Operational Cost:**

The overall operation cost that should be minimized is the cost of generation, trading and penalty of the unsupplied electricity. This can be expressed as equation 26:

$$C_{\text{total}} = \sum_{i=1}^{N} \left(\lambda_i^{\text{MT}} P_{i,t}^{\text{MT}} + \lambda_i^{\text{BS}} P_{i,t}^{\text{BS}} + P_{i,t}^{\text{BSD}} + k_i^{\text{TS}} H_{i,t}^{\text{TSC}} + H_{i,t}^{\text{TSD}}\right) \quad (26)$$

Where, P represents the power at time t from different sources (generation, trading, etc.), $\lambda_i$ are the cost coefficients for each generation source. $K_i$ represents penalty coefficients for unsupplied electricity.

**Power Losses (Active and Reactive Power Losses):**

The network is calculated to make power losses and they are defined as equation 27 and 28:

$$\text{Loss}_{\text{active}} = \sum_{i=1}^{N} P_{i,t}^{\text{loss}} \quad (27)$$

$$\text{Loss}_{\text{reactive}} = \sum_{i=1}^{N} Q_{i,t}^{\text{loss}} \quad (28)$$

Where, $p_i$ is the active power loss at node i and time t. $Q_i$ is the reactive power loss at node i and time t.

**Voltage Deviation:**

Voltage deviation is determined in the individual buses and is determined as a difference between the voltage of the bus and the nominal voltage is presented in equation 29:

$$\text{Voltage Deviation}_{k,t} = | U_{k,t} - U_{\text{nominal}} | \quad (29)$$

Where, $U_{k,t}$ is the voltage at bus k and time t. $U_{\text{nominal}}$ is the nominal voltage value (usually 1 p.u. or another reference value).

**Fitness Function (PSO Optimization):**

The fitness (equation 30) employed in the PSO algorithm is a mix of cost reduction and maximization of resilience:

$$\text{Fitness}(x) = w \cdot \text{Cost}(x) + (1 - w) \cdot \text{Resilience}(x) \quad (30)$$

Where:

- $\text{Cost}(x)$ represents the total cost.
- $\text{Resilience}(x)$is a measure of the system's robustness to uncertainty in renewable generation, which can be represented as equation 31:

$$\text{Resilience}(x) = \text{Var}(\Delta P_{\text{RE}}) \quad (31)$$

Where, $\text{Var}(\Delta \text{PRE})$ is the variance of the uncertainty in renewable energy generation (solar and wind).

SIMULATION RESULTS

Particle Swarm Optimization (PSO) algorithm was developed with the help of MATLAB (R2021b) and its extensive optimization toolbox and big data solutions. The power flow calculations were also done with MATLAB by the Newton-Raphson method, and custom scripts were written to simulate the network. All the information, all calculations, all graphs, voltage profiles, power loss curves, all were handled and analyzed in the environment of MATLAB, which made the implementation comprehensive.

This study used the IEEE 84-bus model of power distribution network, which is a standard of power distribution research. The dataset will contain data about 84 buses and 120 branches and will have initial power injections of 1200 MW. It can also deliver bus information, line impedance (resistance and reactance), switch status to reconfigure and renewable generation (PV and WT) information, including capacity and output. It is possible to simulate the network performance with various configurations due to the data.

In this section, experimental results that have been obtained through the application of advanced optimization techniques to substantially improve the operational efficiency and overall performance of the TPC distribution network under various difficult conditions are presented and discussed. The empirical findings are carefully arranged and presented in three different but incrementally difficult operations to show the progressive improvements as follows.

A baseline is established by analyzing the TPC network's performance under standard operating conditions, without renewables or optimization.

- Complexity is increased by introducing combined PV and WT generation, demonstrating PSO's role in optimizing network performance under variable conditions.
- The integration of PSO-optimized reconfiguration techniques is evaluated, highlighting improvements in power flow, loss reduction, and voltage profile stability.

This structured presentation clearly delineates the advantages, practical implications, and overall contributions of the developed optimization techniques to modern power distribution network management.

**Configuration 1: baseline**

This section contains the main outcomes of simulation results for the TPC distribution network under baseline conditions (Configuration 1). The TPC network was first simulated without considering the

integration of PV and WT renewable energy sources, and also without considering the application of PSO optimization methods. The baseline scenario is intended to provide a quantitative performance standard to measure the future effect of the integration and optimization methods of RES.

*Power Losses Analysis*

Power losses, mainly due to the resistive and reactive nature of the components in the network, is an inherent and very critical aspect of power system operation. Baseline simulations for the TPC distribution network showed that the total active power loss was 4.924 MW. These losses are mostly due to line impedance, transformer inefficiencies, and voltage drops, underscoring the importance of robust system design and efficient operational strategies. In order to maintain high transmission and distribution efficiency, mitigate excessive energy dissipation, and ensure continuous reliability (all of which are critical for grid stability and economic viability), such measures are essential.

*Overall System Cost (Best Cost)*

This section evaluates the baseline operating cost and voltage stability of the TPC network. Under baseline conditions, the optimal operating cost of the TPC distribution network was calculated to be \$6.7931/MWh, which is an important factor in energy system management. Based on the principles of optimal economic dispatch, this measure is the most economical method for reliably meeting demand while taking into account restrictions of the grid, ensuring quality of supply, reliability and economic viability. Fig. 5 shows the voltage profile for various buses, which is an important instrument for evaluating the voltage stability under baseline conditions. This visualization gives very important insight into the intrinsic voltage profile and potential anomalies which can help to identify areas for improvement in the next optimization steps.

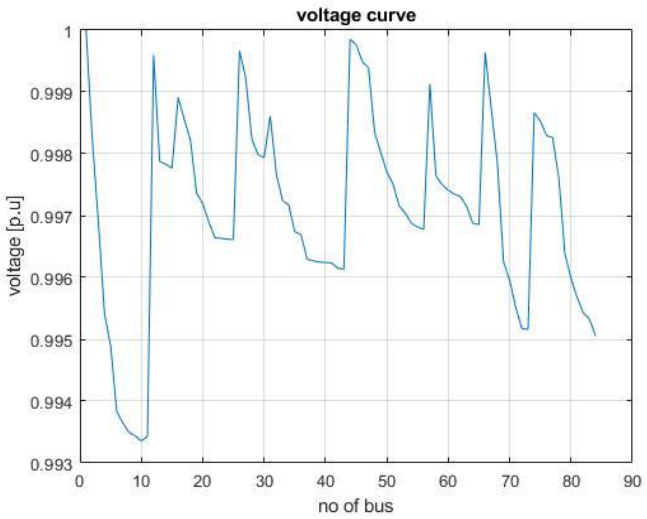


Figure 5. Voltage Profile of the TPC distribution network under baseline operating conditions

**Configuration 2: TPC with renewables and PSO**

This section presents the full results from configuration 2, which is a considerable improvement by combining a hybrid renewable energy portfolio that includes both PV and WT sources. The PSO algorithm is used for the optimization of the TPC network's operational parameters under the integrated renewable energy conditions. Despite the complexity added by the PV and WT integration, the PSO algorithm is able to find the best power injection strategy to keep the grid stable.

*Optimal Placement of PV and WT Systems for Hybrid Integration*

Table 6 shows systematically the optimal bus location for both PV and WT systems in the TPC microgrid segments. This precise and optimized allocation of both PV and WT units is thus a critical enabler A

fundamental aspect of achieving the enhanced performance in configuration 2 is the meticulous determination of optimal placement for both PV and WT distributed generation units. Figure 6 offers a visual representation of the segments of the microgrid and the initial integration points for PV and WT systems to determine the most favorable bus locations for all the renewable energy sources in this hybrid case. Such strategic position is important to maximize the utilization of renewable energies, minimize active power losses, improve voltage profiles and enhance overall grid stability under variable generation conditions for the efficient and reliable operation of TPC network under high penetration of diversified renewable energy.

*Power Losses, Cost Optimization, and Voltage Profile Enhancement*

This section analyses the performance of TPC's distribution network under configuration 2 which reveals substantial gains following the optimal incorporation of both PV and WT systems, drastic reduction was observed in respect of energy losses and operational costs with respect to the baseline values. The PSO algorithm was repeated 200 times so that the optimal energy configuration can be reached, and its convergence performance is plotted on Figure 7. For the case of cost, the optimization started from 9.0 \$/MWh and fell steeply to 5.0 \$/ MWh in the first iteration and then converged at optimal 2.1011 \$/MWh after nearly 140 iterations, thereby confirming the ability of PSO in solving complex problems over an enlarged solution space. As shown in Figure 8, and the voltage profile in Figure. When compared with the un-optimized baseline, the total active powers losses have been achieved significantly from 4.924 to 0.0021 MW meanwhile. The main key performance indicators results are listed in Table 7, which indicates the efficient integration of hybrid renewable energy is achieved with PSO optimization. Overall, these findings unambiguously reveal a significant cost-effectiveness improvement in voltage stability and power loss reduction for the integration of hybrid PV-WT systems into the TPC network through PSO-best methodology.

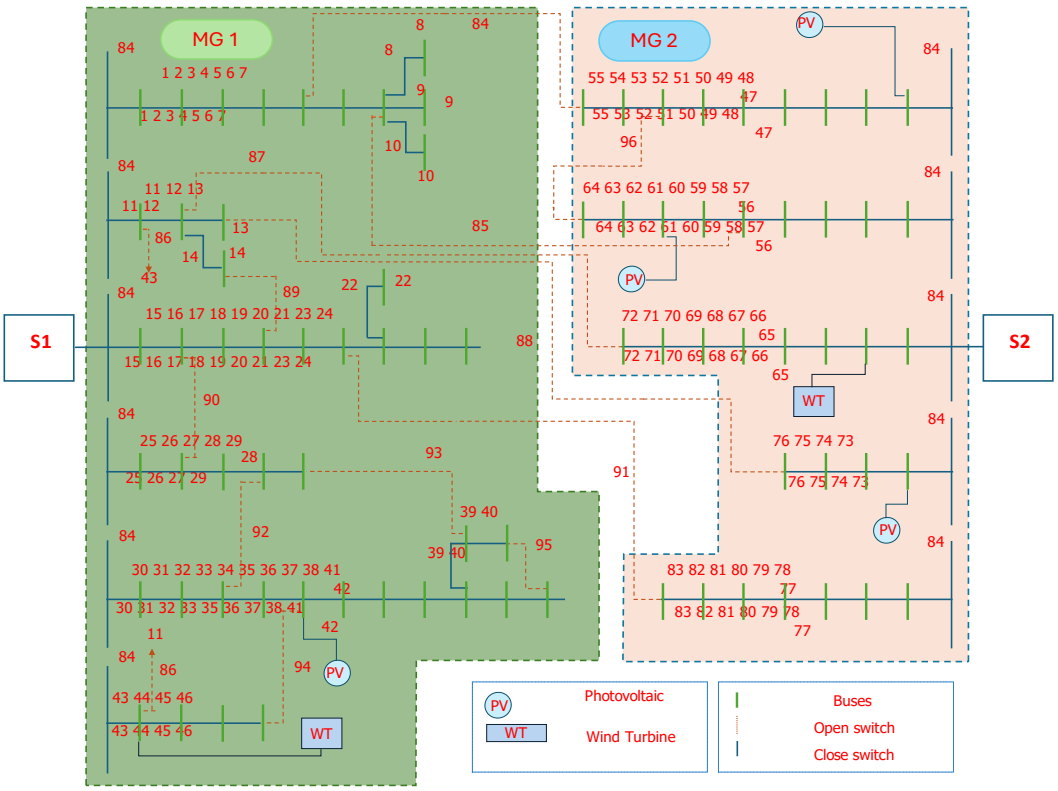


Figure 6. Schematic Diagram of the IEEE 84-Bus TPC Distribution Network, illustrating the optimized topology with MG1 and MG2 segments, alongside the strategic placement of integrated PV and WT generation systems.

Table 6. Optimal placement locations for PV and WT systems within the TPC distribution network microgrids

| Microgrid Segment | Bus Number (PV / WT Location) |
|---|---|
| MG 1 (Green) | Bus 42 - PV |
| MG 1 (Green) | Bus 44 - WT |
| MG 2 (Yellow) | Bus 84 - PV |
| MG 2 (Yellow) | Bus 60 - PV |
| MG 2 (Yellow) | Bus 84 - WT |
| MG 2 (Yellow) | Bus 34 - PV |
| MG 2 (Yellow) | Bus 43 - WT |
| MG 2 (Yellow) | Bus 46 - PV |

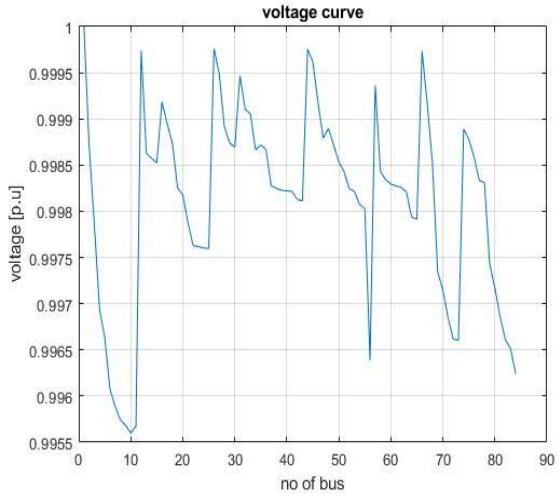


Figure 7. Convergence curve of the PSO algorithm for hybrid PV-WT integration

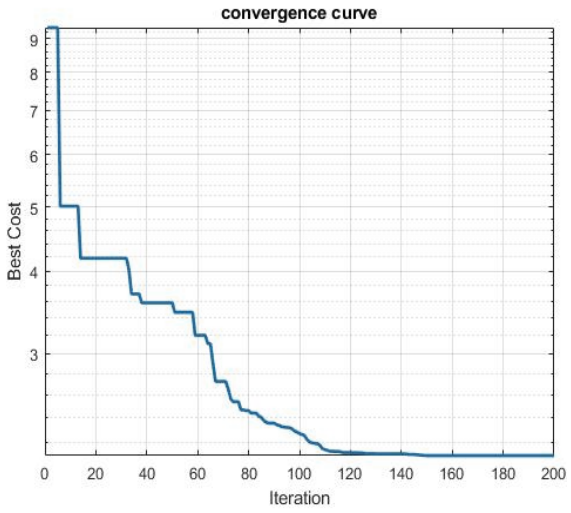


Figure 8. Per-Unit Voltage Profile of the TPC Distribution Network under Optimized Hybrid PV-WT Integration

Table 7. Key performance indicators and PSO algorithm parameters for the TPC distribution network under optimized hybrid PV-WT integration

| Parameter | Value |
|---|---|
| Number of Iterations | 200 |
| Best Cost ($/MWh) | 2.1011 |
| Total Power Losses (MW) | 0.0021 |
| Number of Search Agents | 10 |

**Configuration 3: Network Reconfiguration**

This section presents a thorough analysis of the performance of the TPC distribution network under Configuration 3 that provides an introduction to the reconfiguration of the network dynamically. The combined integration of distributed generation and network reconfiguration is expected to provide a better performance than the previous configurations. Detailed findings and discussions will discuss network reconfiguration scheme and topology, and further analysis of power losses and cost optimization, convergence analysis, enhanced voltage profile, and overall performance comparison.

*Network Reconfiguration Scheme and Topology*

This subsection explains how to strategically reconfigure the switches to change the flow of power and increase the thermal efficiency. The resulting optimized network topology, which is a visual representation of changed switch states and MG1 and MG2 delineation, is shown in Figure 9. Optimal switch locations in order to minimize losses and maximize efficiency are systematically given in Table 8. The implementation of coordinated reconfiguration, in addition to the continued PV and WT integration led to significant extra reductions in both energy losses and operational costs.

*Power Losses, Cost Optimization, and Voltage Profile Enhancement*

As shown in the convergence curve shown in Figure 10, the optimization process started with the initial best cost of \$8.0/MWh, and quickly lowered to 5.2 \$/MWh, and settled on a very low value of only 1.954 \$/MWh by iteration 120, proving better economic performance. A direct comparison with the results obtained for Configuration 2 indicates that the total power losses were further decreased from 0.0021 MW to 0.002 MW and the best cost was improved from 2.1011 \$/MWh to 1.954 \$/MWh. Compared with the baseline system without the integration of renewables, the power losses were greatly reduced from 4.924 MW to only 0.002 MW, which undoubtedly demonstrated the dramatic improvements in energy efficiency and cost-effectiveness. Figure 11 shows the improved stability of voltage with the voltage profile showing minimum fluctuations over the system buses. The culmination of all these performance indicators is summarized in Table 9. The synergistic integration of PV and WT systems with strategic network reconfiguration certainly presents the best performance of all tested configurations, which can be considered as an important strategy to optimal cost and loss reduction for modern energy distribution systems.

Table 8. Optimal placement locations for PV systems within the TPC distribution network microgrids

| Microgrid Segment | Bus Number (PV Location) |
|---|---|
| MG 1 (Green) | Bus 12 |
| MG 1 (Green) | Bus 20 |
| MG 1 (Green) | Bus 29 |
| MG 1 (Green) | Bus 31 |
| MG 1 (Green) | Bus 43 |
| MG 1 (Green) | Bus 36 |
| MG 1 (Green) | Bus 55 |
| MG 2 (yellow) | Bus 52 |
| MG 2 (yellow) | Bus 62 |
| MG 2 (yellow) | Bus 70 |
| MG 2 (yellow) | Bus 79 |

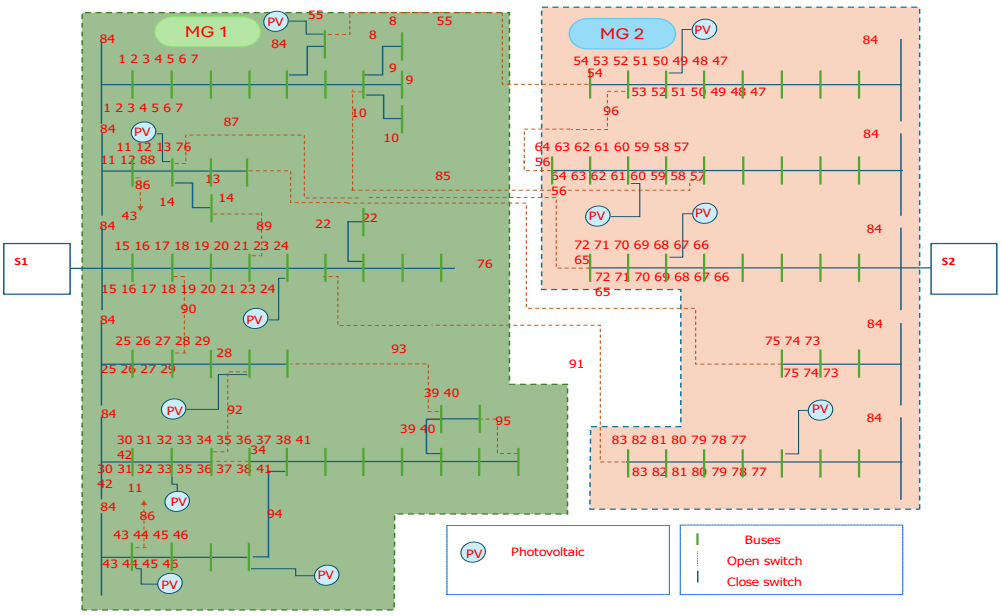


Figure 9. Reconfigured topological representation of the TPC distribution network with integrated PV systems and microgrid segmentation

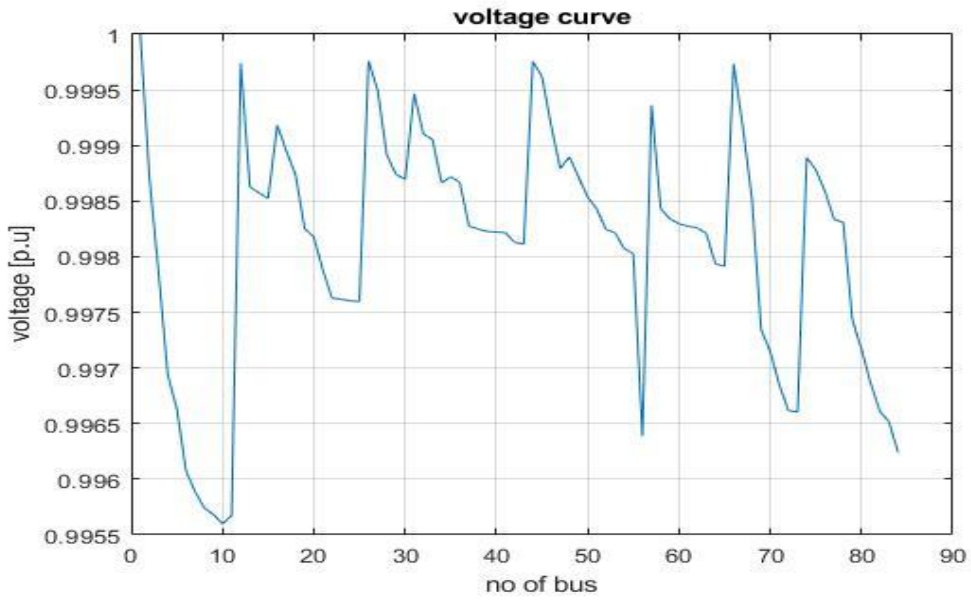


Figure 10. Convergence Curve of the PSO algorithm for PV, WT Integration with Network Reconfiguration

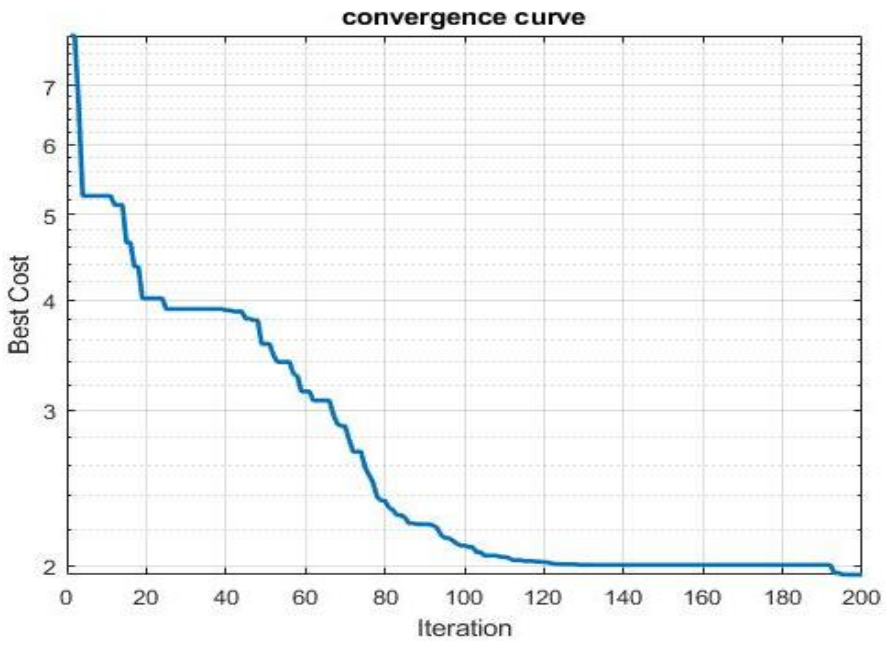


Figure 11. Per-Unit Voltage Profile of the TPC Distribution Network under Optimized PV, WT Integration with Network Reconfiguration

Table 9. key performance indicators and PSO algorithm parameters for the TPC distribution network under optimized PV, WT integration with network reconfiguration

| Parameter | Value |
|---|---|
| Number of Iterations | 200 |
| Best Cost ($/MWh) | 1.954 |
| Total Power Losses (MW) | 0.002 |
| Number of Search Agents | 10 |

DISCUSSION

This study offered a thorough comparative analysis of several power distribution network configurations with significant beneficial aspects of incorporating renewable energy systems with dynamic grid reconfiguration. The main objective was to obtain an optimal energy trading scheme within the power

distribution network, and the results always prove the excellent performance of this advanced configuration on the aspects of voltage stability, power loss reduction and total cost reduction. One of the most important ones is the significant improvement in voltage stability achieved by strategic reconfiguration of the network.

Table 10. Comparative performance evaluation of key optimal metrics for different system configurations

| Parameter | PV and WT (Configuration 2) | PV and WT, Reconfiguration (Configuration 3) |
|---|---|---|
| Best Cost ($/MWh) | 2.1011 | 1.954 |
| Total Losses (MW) | 0.0021 | 0.0020 |
| NO of Search Agents | 10 | 10 |
| Iterations | 200 | 200 |

The multi-stage optimization process consistently showed that energy trading augmented with network reconfiguration represents the most optimal methodology. This configuration yielded the best results in terms of cost-effectiveness, substantial power loss reduction, and superior voltage regulation. The final optimized scenario achieved the lowest recorded operational cost of $1.954/MWh and remarkably reduced total active power losses to 0.002 MW. These figures represent a drastic improvement compared to the initial baseline system without renewable integration or optimization, where power losses were as high as 4.924 MW and operational costs were significantly greater. The comparative analysis of two distinct configurations, standard PV-WT integration versus reconfigured PV-WT operation, revealed a clear progression in performance improvements. The reconfigured PV-WT system exhibited the fastest convergence rate and achieved the lowest operational cost, proving to be the most efficient and optimal solution. Further detailed performance evaluations of these configurations, including best cost and total power losses, are systematically presented in Table 10. This table robustly confirms the superiority of the reconfiguration approach, as it consistently provided the minimum best operational cost of $1.954/MWh and achieved the lowest total power losses of 0.0020 MW.

## CONCLUSION

This study proves that combining the hybrid photovoltaic (PV) and wind turbine (WT) generation systems with dynamic network reconfiguration can greatly improve the performance of the modern distribution networks. The suggested method is quite effective to lower the operation costs and the lost power, enhance the voltage stability and network performance. To be more precise, the outcomes of optimization revealed that operational costs (minimized to $6.7931/MWh at baseline) decreased to 1.954/MWh in the final structure, whereas the power losses dropped to 0.002 MW, which is a drastic drop in comparison to 4.924 MW. These gains justify the fact that the suggested strategy can result in energy distribution optimization and achieve optimal smart grid efficiency. The statistical results proved the advantage of the PSO-based optimization, in which 200 iterations of the algorithm are convergent and optimal metrics of the cost and power losses are in proper agreement with optimal network operation. The voltage profiles also demonstrated the increased stability with the integrated hybrid renewable energy setup, with the significance of the best location and rearrangement of the grid elements. The proposed research may be extended in future studies by using real-time data and adaptive control systems, which would enhance the ability of the grid to react to changes in the amount of renewable energy generated. Also, the addition of energy storage systems might be considered as the next higher step in flexibility, as well as decrease intermittency and the system stability and reliability on the whole. Lastly, multi-objective optimization frameworks might also be useful to add other considerations like environmental impact, grid resilience and cost-effectiveness to guarantee a more holistic approach towards optimization of smart grid environments.

REFERENCES


[1] Arévalo P, Ochoa-Correa D, Villa-Ávila E, Iñiguez-Morán V, Astudillo-Salinas P. Systematic Review of Hierarchical and Multi-Agent Optimization Strategies for P2P Energy Management and Electric Machines in Microgrids. Applied Sciences. 2025 Apr 26;15(9):4817. https://doi.org/10.3390/app15094817

[2] Alarcon-Rodriguez A, Ault G, Galloway S. Multi-objective planning of distributed energy resources: A review of the state-of-the-art. Renewable and Sustainable Energy Reviews. 2010 Jun 1;14(5):1353-66. https://doi.org/10.1016/j.rser.2010.01.006

[3] Aznavi S, Fajri P, Shadmand MB, Khoshkbar-Sadigh A. Peer-to-peer operation strategy of PV equipped office buildings and charging stations considering electric vehicle energy pricing. IEEE Transactions on Industry Applications. 2020 Apr 27;56(5):5848-57. https://doi.org/10.1109/TIA.2020.2990585

[4] Cui S, Xu S, Hu F, Zhao Y, Wen J, Wang J. A consortium blockchain-enabled double auction mechanism for peer-to-peer energy trading among prosumers. Protection and Control of Modern Power Systems. 2024 Mar 26;9(3):82-97. https://doi.org/10.23919/PCMP.2023.000038

[5] Boumaiza, A. (2024). A blockchain-based scalability solution with microgrids peer-to-peer trade. Energies, 17(4), 915.

[6] Hafeez G, Wadud Z, Khan IU, Khan I, Shafiq Z, Usman M, Khan MU. Efficient energy management of IoT-enabled smart homes under price-based demand response program in smart grid. Sensors. 2020 Jun 2;20(11):3155. https://doi.org/10.3390/s20113155

[7] Teotia F, Mathuria P, Bhakar R. Peer-to-peer local electricity market platform pricing strategies for prosumers. IET Generation, Transmission & Distribution. 2020 Oct;14(20):4388-97. https://doi.org/10.1049/iet-gtd.2019.0578

[8] Zhou Y, Wu J, Long C, Ming W. State-of-the-art analysis and perspectives for peer-to-peer energy trading. Engineering. 2020 Jul 1;6(7):739-53. https://doi.org/10.1016/j.eng.2020.06.002

[9] Zhou B, Zou J, Chung CY, Wang H, Liu N, Voropai N, Xu D. Multi-microgrid energy management systems: Architecture, communication, and scheduling strategies. Journal of Modern Power Systems and Clean Energy. 2021 May;9(3):463-76. https://doi.org/10.35833/MPCE.2019.000237

[10] Machele IL, Onumanyi AJ, Abu-Mahfouz AM, Kurien AM. Interconnected smart transactive microgrids—A survey on trading, energy management systems, and optimisation approaches. Journal of Sensor and Actuator Networks. 2024 Mar 1;13(2):20. https://doi.org/10.3390/jsan13020020

[11] Wang Y, Huang Z, Shahidehpour M, Lai LL, Wang Z, Zhu Q. Reconfigurable distribution network for managing transactive energy in a multi-microgrid system. IEEE transactions on smart grid. 2019 Aug 15;11(2):1286-95. https://doi.org/10.1109/TSG.2019.2935565

[12] Saatloo AM, Mirzaei MA, Mohammadi-Ivatloo B. A robust decentralized peer-to-peer energy trading in community of flexible microgrids. IEEE Systems Journal. 2022 Sep 7;17(1):640-51. https://doi.org/10.1109/JSYST.2022.3197412

[13] Kabirifar M, Fotuhi-Firuzabad M, Moeini-Aghtaie M, Pourghaderi N, Dehghanian P. A bi-level framework for expansion planning in active power distribution networks. IEEE Transactions on Power Systems. 2021 Nov 24;37(4):2639-54. https://doi.org/10.1109/TPWRS.2021.3130339

[14] Li J, Xu D, Wang J, Zhou B, Wang MH, Zhu L. P2P multigrade energy trading for heterogeneous distributed energy resources and flexible demand. IEEE Transactions on Smart Grid. 2022 Jun 9;14(2):1577-89. https://doi.org/10.1109/TSG.2022.3181703

[15] Misra S, Panigrahi PK, Ghosh S, Dey B. Economic operation of a microgrid system with renewables considering load shifting policy. International Journal of Environmental Science and Technology. 2024 Feb;21(3):2695-708. https://doi.org/10.1007/s13762-023-05125-y

[16] Zou Y, Xu Y, Feng X, Nguyen HD. Peer-to-peer transactive energy trading of a reconfigurable multi-energy network. IEEE Transactions on Smart Grid. 2022 Nov 21;14(3):2236-49. https://doi.org/10.1109/TSG.2022.3223378

[17] Yan M, Shahidehpour M, Paaso A, Zhang L, Alabdulwahab A, Abusorrah A. Distribution network-constrained optimization of peer-to-peer transactive energy trading among multi-microgrids. IEEE transactions on smart grid. 2020 Oct 22;12(2):1033-47. https://doi.org/10.1109/TSG.2020.3032889

[18] Feng C, Liang B, Li Z, Liu W, Wen F. Peer-to-peer energy trading under network constraints based on generalized fast dual ascent. IEEE Transactions on Smart Grid. 2022 Mar 29;14(2):1441-53. https://doi.org/10.1109/TSG.2022.3162876

[19] Zhao W, Zhang S, Xue L, Chang T, Wang L. Research on model of micro-grid green power transaction based on blockchain technology and double auction mechanism. Journal of Electrical Engineering & Technology. 2024 Jan;19(1):133-45. https://doi.org/10.1007/s42835-023-01541-9

[20] Borokhov V. Modified convex hull pricing for fixed load power markets. Energy Systems. 2023 Nov;14(4):1107-34. https://doi.org/10.1007/s12667-022-00525-4

[21] AlAshery MK, Yi Z, Shi D, Lu X, Xu C, Wang Z, Qiao W. A blockchain-enabled multi-settlement quasi-ideal peer-to-peer trading framework. IEEE Transactions on Smart Grid. 2020 Sep 8;12(1):885-96. https://doi.org/10.1109/TSG.2020.3022601

[22] Ma H, Xiang Y, Sun W, Dai J, Zhang S, Liu Y, Liu J. Optimal peer-to-peer energy transaction of distributed prosumers in high-penetrated renewable distribution systems. IEEE Transactions on Industry Applications. 2024 Jan 23;60(3):4622-32. https://doi.org/10.1109/TIA.2024.3357790

[23] Kahouli O, Alsaif H, Bouteraa Y, Ben Ali N, Chaabene M. Power system reconfiguration in distribution network for improving reliability using genetic algorithm and particle swarm optimization. Applied Sciences. 2021 Mar 31;11(7):3092. https://doi.org/10.3390/app11073092

[24] Nyingu BT, Masike L, Mbukani MW. Multi-Objective Optimization of Load Flow in Power Systems: An Overview. Energies. 2025 Nov 20;18(22):6056. https://doi.org/10.3390/en18226056

[25] An S, Wang H, Leng X. Optimal operation of multi-micro energy grids under distribution network in Southwest China. Applied Energy. 2022 Mar 1;309:118461. https://doi.org/10.1016/j.apenergy.2021.118461

[26] Tostado-Véliz M, Kamel S, Hasanien HM, Turky RA, Jurado F. Uncertainty-aware day-ahead scheduling of microgrids considering response fatigue: An IGDT approach. Applied Energy. 2022 Mar 15;310:118611. https://doi.org/10.1016/j.apenergy.2022.118611

[27] Umar A, Kumar D, Ghose T. Decentralized energy trading in microgrids: a blockchain-integrated model for efficient power flow with social welfare optimization. Electrical Engineering. 2025 Mar;107(3):2677-95. https://doi.org/10.1007/s00202-024-02635-x

[28] Tarnate WR, Ponci F, Monti A. Uncertainty-aware model predictive control for residential buildings participating in intraday markets. IEEE Access. 2022 Jan 6;10:7834-51. https://doi.org/10.1109/ACCESS.2022.3140598

[29] Nazemi M, Dehghanian P, Lu X, Chen C. Uncertainty-aware deployment of mobile energy storage systems for distribution grid resilience. IEEE Transactions on Smart Grid. 2021 Mar 8;12(4):3200-14. https://doi.org/10.1109/TSG.2021.3064312

[30] Ahmed M, Khan MR. Artificial intelligence-enabled digital twins for energy efficiency in smart grids. Review of Applied Science and Technology. 2025 Aug 5;4(02):580-615. https://doi.org/10.63125/12kp9w74

[31] Zare K, Akbari-Dibavar A, Najafi Ravadanegh S, Vahidinasab V. Resiliency-oriented scheduling of multi-microgrids in the presence of fuel cell-based mobile storage using hybrid stochastic-robust optimization. Journal of Energy Management and Technology. 2024 Dec 1;8(4):307-20. https://doi.org/10.22109/jemt.2024.441626.1487

[32] Ghias-Nodoushan A, Sedighi-Anaraki A, Jannesar MR, Saeedi-Sourck H. Optimizing solar farm interconnection networks using graph theory and metaheuristic algorithms with economic and reliability analysis. Scientific Reports. 2025 Sep 26;15(1):33114. https://doi.org/10.1038/s41598-025-18108-5

[33] Gharehveran SS, Shirini K, Khavar SC, Mousavi SH, Abdolahi A. Deep learning-based demand response for short-term operation of renewable-based microgrids. The Journal of Supercomputing. 2024 Dec;80(18):26002-35. https://doi.org/10.1007/s11227-024-06407-z

[34] Perez-Flores AC, Antonio JD, Olivares-Peregrino VH, Jiménez-Grajales HR, Claudio-Sanchez A, Ramírez GV. Microgrid energy management with asynchronous decentralized particle swarm optimization. IEEE Access. 2021 May 7;9:69588-600. https://doi.org/10.1109/ACCESS.2021.3078335

[35] Alanazi A, Alanazi M, Memon ZA, Awan AB, Deriche M. Availability and uncertainty-aware optimal placement of capacitors and DSTATCOM in distribution network using improved exponential distribution optimizer. Scientific Reports. 2025 Apr 16;15(1):13204. https://doi.org/10.1038/s41598-025-87139-9

[36] Chen P, Liu S, Wang X, Kamwa I. Physics-guided multi-agent deep reinforcement learning for robust active voltage control in electrical distribution systems. IEEE Transactions on Circuits and Systems I: Regular Papers. 2023 Dec 14;71(2):922-33. https://doi.org/10.1109/TCSI.2023.3340691

[37] Zhang Y, Tian J, Guo Z, Fu Q, Jing S. Uncertainty-Aware Economic Dispatch of Integrated Energy Systems with Demand-Response and Carbon-Emission Costs. Processes. 2025 Jun 16;13(6):1906. https://doi.org/10.3390/pr13061906

[38] Zahraoui Y, Korõtko T, Rosin A, Zidane TE, Agabus H, Mekhilef S. A Competitive Framework for the participation of Multi-Microgrids in the community Energy Trading Market: A case Study. IEEE Access. 2024 May 8;12:68232-48. https://doi.org/10.1109/ACCESS.2024.3399168

[39] Samy MM, Elkhouly HI, Barakat S. Multi-objective optimization of hybrid renewable energy system based on biomass and fuel cells. International Journal of Energy Research. 2020 Sep 24 ;45(6):8214–8230. https://doi.org/10.1002/er.5815

[40] Wei Z, Jia B, Dong X, Li F, Sun B. Knowledge-driven multi-timescale optimization dispatch for hydrogen-electricity coupled microgrids. International Journal of Hydrogen Energy. 2025 Apr 17;120:333-45. https://doi.org/10.1016/j.ijhydene.2025.03.274

[41] Hu W, Yang Q, Yuan Z, Yang F. Wind farm layout optimization in complex terrain based on CFD and IGA-PSO. Energy. 2024 Feb 1;288:129745. https://doi.org/10.1016/j.energy.2023.129745

[42] Ebrahimi H, Shahnia F, Nikdel N, Galvani S. Renewable energy and demand uncertainty-aware stochastic allocation and management of soft open points for simultaneous reduction of harmonic distortion, voltage deviations and losses. Computers and Electrical Engineering. 2025 Apr 1;123:110208. https://doi.org/10.1016/j.compeleceng.2025.110208

[43] Zhu C, Zhang S. An adaptive uncertainty-aware hybrid neural network for enhanced learning in real-time building energy prediction with dynamic occupant behavior modeling. Intelligent Decision Technologies. 2025 Nov 12;19(6):3776–3803. https://doi.org/10.1177/18724981251389334.

[44] Wang T, Liu H, Su M. Energy Optimization for Microgrids Based on Uncertainty-Aware Deep Deterministic Policy Gradient. Processes. 2025 Apr 1;13(4):1047. https://doi.org/10.3390/pr13041047

[45] Patnaik S, Nayak MR, Viswavandya M. Smart deployment of energy storage and renewable energy sources for improving distribution system efficacy. AIMS Electronics and Electrical Engineering. 2022;6(4):397-417. http://dx.doi.org/10.3934/electreng.2022024